engineering proceedings

MDPI

Proceeding Paper

Design of Photonic Crystal Fiber for 5G Communication Using COMSOL Multiphysics †

Sandip Das [1]*, Riya Sen[2]

[1] Geetanjali Institute of Technical Studies, Udaipur, India; info.sandipec@gmail.com
[2] Geetanjali Institute of Technical Studies, Udaipur, India; riyasen4130@gmail.com
* Correspondence: info.sandipec@gmail.com;

† The 4th International Electronic Conference on Applied Sciences (ASEC2023), online, and 27 October–10 November 2023.

Abstract: Photonic crystal fibers (PCFs) have emerged as promising candidates for enabling high-performance 5G communication systems, attributed to their low loss and wide bandwidth characteristics. In this research, we leverage the capabilities of COMSOL Multiphysics software to meticulously design a novel photonic crystal fiber (PCF) design based on Topas, featuring a rectangular air gap core with integrated slots, surrounded by a cladding composed of circular and octagon air holes. The circular air holes are arranged in square and octagon lattice structures, while the octagon air holes form a rhombic lattice. The proposed structure exhibits a high birefringence of 0.05 and low effective material loss (EML) of 0.059 cm^{-1} and 0.057 cm^{-1} at 2THz for x and y polarization mode respectively. Moreover, the proposed waveguide also has a low confinement loss of 10^{-10} and 10^{-11} cm^{-1} for x and y polarization mode. Thus, the proposed PCF structure exhibits significant potential for facilitating 5G requirements.

Keywords: Photonic crystal fiber, 5G communication, Terahertz, Photonics, optical communication

1. Introduction

The 5G spectrum requires a mix of frequency bands to cater to various use cases. Lower frequency bands (sub-6 GHz) offer wide area coverage and obstacle penetration, while higher frequency bands (millimeter-wave bands like 28 GHz, 39 GHz, and 60 GHz) provide vast spectrum and high data rates but with reduced coverage and susceptibility to blockages. Exploring Terahertz (THz) frequencies, ranging from 0.1 to 10 THz, has become a groundbreaking avenue for enhancing communication capabilities in next-generation wireless networks. Ultra-wideband transmission demands the inclusion of THz or sub-THz bands, resulting in shorter wireless paths and improved fiber penetration. Both wireless and optical technologies play significant roles beyond the 5G communication era.

Terahertz (THz) radiation's extensive frequency range has non-ionizing properties and low energy, making it suitable for penetrating non-polar and non-conductive materials [1]. This characteristic enables diverse applications, including sensing, spectroscopy, medical diagnostics, security screening, imaging, and communication systems [2-3]. Traditional THz systems have been large and relied on free-space propagation, leading to challenges like water vapor absorption loss, material loss, and misalignment between transmitters and receivers [4-5]. To address these issues, waveguides offer a critical solution for low loss and low dispersion THz wave propagation.

Waveguides aim to efficiently transmit electromagnetic radiation with minimal loss across various wavelengths. Metallic waveguides suffer from THz radiation absorption and bending losses [6-7]. Dielectric waveguides, like classic optical fibers, show promise for higher frequencies, categorized as solid, porous, or hollow-core fibers based on their

Citation: To be added by editorial staff during production.

Academic Editor: Firstname Lastname

Published: date

guiding mechanisms [8]. Solid-core fibers have higher absorption loss than hollow-core fibers [9], but the latter are limited to a narrow frequency band, unlike the broader THz spectrum.

An alternative approach is the development of photonic crystal fibers (PCFs), wherein a solid core is inserted with micro-structured air holes [10]. The utilization of air as a non-absorbent medium in this fiber design results in several advantageous characteristics, including reduced material loss, enhanced transmission efficiency, and lower bending loss. Moreover, the fiber exhibits high birefringence and offers flexibility in modifying its guiding properties by controlling geometrical parameters.

Researchers extensively studied optical and chemical properties of various materials for THz waveguides [11]. Commonly employed materials include polymethyl methacrylate, high-density polyethylene plastic, Teflon, Topas, and Zeonex. Topas is preferred due to its low material absorption loss, constant refractive index across a broad frequency range (0.1–2 THz), humidity insensitivity, and versatility in biosensing and photosensitive applications [12-13]. Its compatibility with Zeonex allows for step-index fiber fabrication, making Topas highly promising for advancing THz communication technologies.

Several notable Photonic Crystal Fibers (PC-PCFs) with exceptional guiding properties, including low Effective Mode Loss (EML), low confinement loss, and high-power fraction within porous air holes are studied by different researchers. For instance, a microstructured polymer fiber, utilizing a hexagonal array of porous air holes, achieved an impressively low EML of 0.018 cm^{-1} at 0.5 THz [14]. Similarly, Uthman et al. proposed another PC-PCF with hexagonal lattice porous air holes, reducing bulk absorption loss of the background material by about 60%. Moreover, Tsuruda et al. introduced a silicon photonic-crystal slab waveguide with remarkably low propagation loss of 0.04 dB/cm at 0.33 THz.

By exploring and optimizing these PCF waveguide technologies, the efficient and low-loss transmission of THz waves becomes increasingly achievable, opening the door to transformative applications in wireless communication and beyond the 5G era. The paper is organized as: In section 2, the designed of the proposed PCF is discussed elaborately. Section 3 presents the results and finally the paper is concluded in section 4.

2. Design of proposed PCF structure

The cross-sectional view of the proposed PCF design is shown in figure 1 (a). The octagon shape air holes forms the outer cladding of the rhombic shaped lattice (lattice 3 and lattice 4) as shown in figure 1 (b). The diameter of the inner circular air hole adjacent to the core is d_1 and the circular air hole in the exterior layer has a diameter d_2. The inner air holes are forms a square lattice (lattice 2) and the outer air holes are arranged in an octagonal shaped lattice (lattice 1) as shown in figure 1 (b). The core consists of 13 rectangular slots of air holes, which forms a shape of octagon having diameter d_{core}. The dimension of the rectangular air holes has length 'L', width 'W' and each rectangular slot is separated by distance known as pitch 'Λ'. Except the three center slots having length 'L' and four slots at the end (in both sides) having length 'L_4', the length of each of the remaining rectangular slots reduces in either side. The length of the rectangular slots decreasing in either side is represented as L_1, L_2 and L_3. Four rectangular slots of length 'L_4' and width 'W' are placed in between two octagon shaped air holes above and below the core as shown in figure 1 (a). The dimensions are listed in table 1.

The finite element method (FEM) based COMSOL v5.6 software is used to simulate the proposed PCF. For the entire simulation process user-controlled mesh is selected for utmost precision. The entire structure was represented by 14382 triangular components and 220 vertex elements. In order to map the varying diameters of the air holes, the minimum element size was set at $0.09\mu m$. The minimum element quality obtained is 0.3914. The mesh representation of the structure is shown in figure 2.

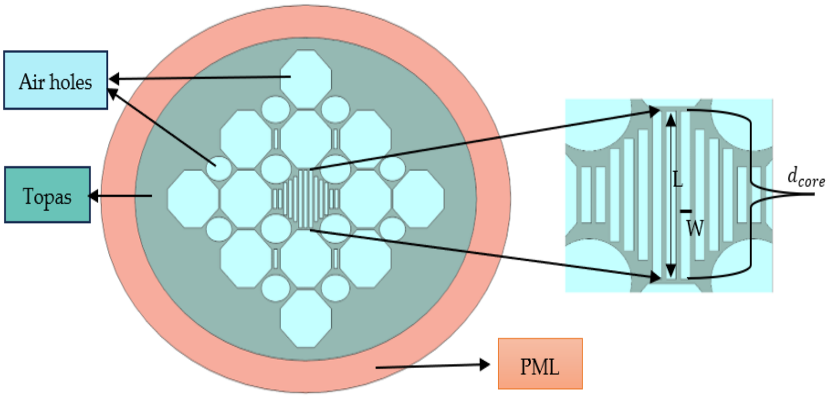

(a) Cross-Section View of the proposed PCF

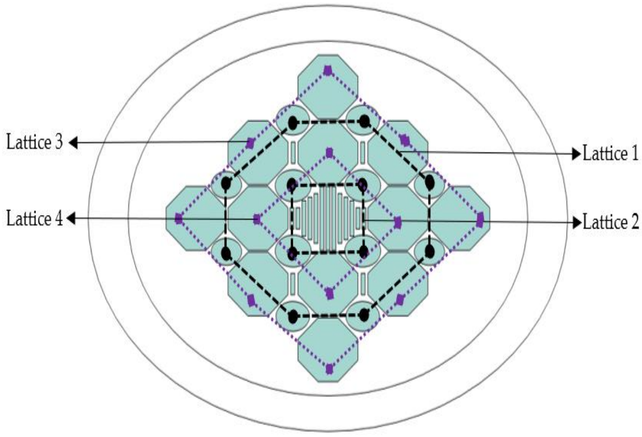

(b) Representation of Lattice formed by circular air holes and octagon air holes

Figure 1. Proposed structure of PCF

The cladding region of the PCF is surrounded by a protective layer that uses the Perfectly Matched Layer (PML) boundary condition. This layer not only ensures simulation accuracy but also effectively eliminates ambient reflections, improving results precision. The structure's background material is topaz, with a refractive index of 1.528 that remains constant throughout a frequency range of 0.1-2 THz.

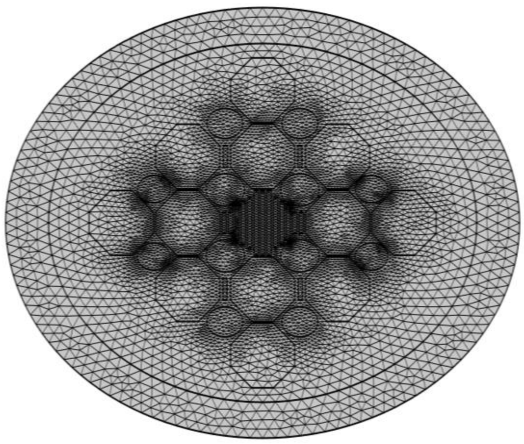

Figure 2. Mesh representation of the proposed PCF structure

Table 1. Dimension of the proposed PCF air holes.

Shape	Dimension
Inner air hole diameter, d_1	90µm
Outer air hole diameter, d_2	76µm
Core diameter, d_{core}	180µm
pitch, Λ	5µm
Width of rectangular core, W	10µm
Length of rectangular slots, L_1, L_2, L_3, L_4	140µm, 120µm, 100µm,60µm

3. Results and Discussions

The proposed PCF is numerically analyzed by utilizing the finite element method. Various PCF characteristics namely birefringence, effective refractive index, effective material loss (EML), confinement loss (CL), effective area and V-parameter, dispersion properties are analyzed to study the performance of the PCF in THz range. In figure 3 the profiles for mode field covering both x-pol and y-pol are represented.

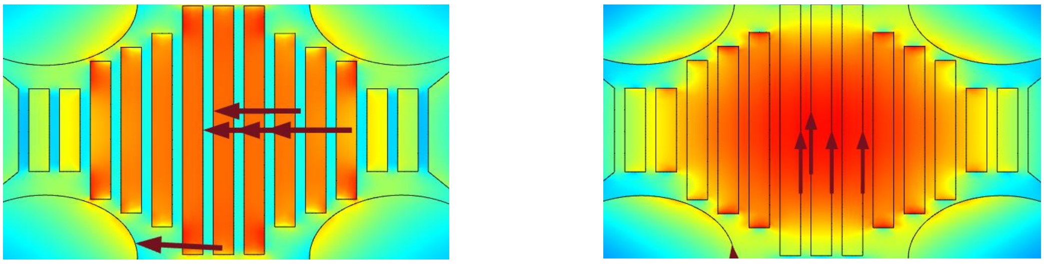

(a) (b)

Figure 3. Fundamental mode field distributions of the proposed PCF at 1 THz (a) x-pol (b) y-pol

3.1. Effective Refractive Index

The effective refractive index of the proposed PCF in correlation with the frequency is depicted in figure 4 for both x-pol and y-pol. As the frequency increases, the fiber's effective refractive index also rises, as shown in figure 4 (a). Higher frequencies cause the mode power to extend into the cladding region, further increasing the effective refractive index. At 2 THz, the suggested fiber exhibits effective refractive indices of approximately 1.1014 for x-polarization and 1.1537 for y-polarization. It is found that the effective refractive index for y-polarization is higher when compared to x-polarization. The y-polarization is chosen as the primary mode since the confinement of light in the core is stronger.

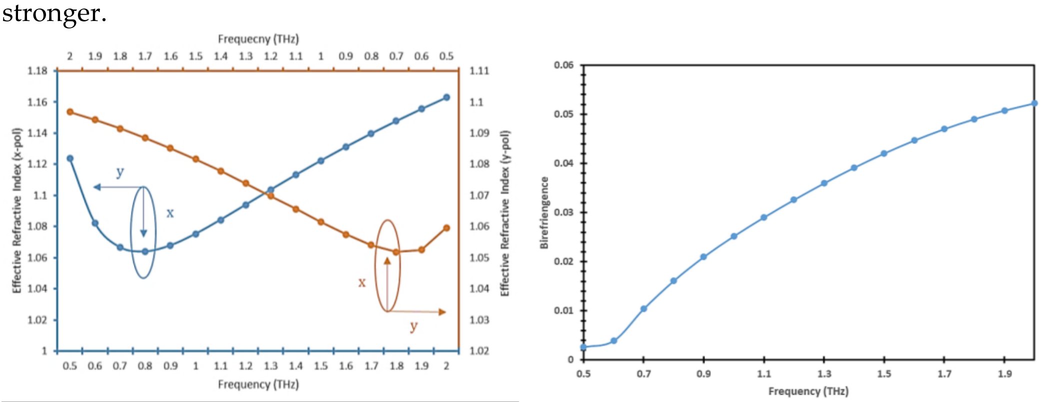

(a) (b)

Figure 4. Graphical representation of (a) effective refractive index vs frequency for x-pol and y-pol (b) Birefriengence versus frequency

3.2. Birefringence

The difference between the refractive indices of two orthogonally polarized modes is termed as birefriengence and it is expressed using the following equation.

$$B = |\eta_x - \eta_y| \quad (1)$$

Where, B represents birefriengence and η_x and η_y represents the respective refractive index of x and y polarised modes. From figure 4 (b) it is clearly seen that birefriengence rises with the increase in frequency upto 1.5 THz and starts to reduce or flatten after 1.5 THz. The higher refractive index gap between the core and the cladding can explain the rise in effective refractive index at high frequencies.

3.3. Effective matrial loss and confinement loss

Terahertz waves propagating through the PCF mostly suffers from effective material loss (EML) or simply known as material absorption loss (α_{eff}). The EML for the proposed PCF can be expressed as follows:

$$\alpha_{eff} = \sqrt{\frac{\varepsilon_0}{\mu_0}}\left(\frac{\int_{mat} \eta_{mat}|E|^2 \alpha_{mat} dA}{|\int_{all} S_z dA|}\right) \quad (2)$$

Where, ε_0 and μ_0 are the relative permittivity and permeability of the vacuum, η_{mat} is the refractive index of the material and α_{mat} denotes the absorption loss of the bulk material. S_z denotes the z-component of the poynting vector which is in the direction of the electromagnetic wave transmission. From figure 5 it is seen that the EML keeps rising with the increase of frequency. It is seen from the figure that for x-polarization mode EML is more compared to y-polarization mode as the frequency increases. In both the modes EML is less for lower frequencies as the confinement of EM wave is more concentrated in the core.

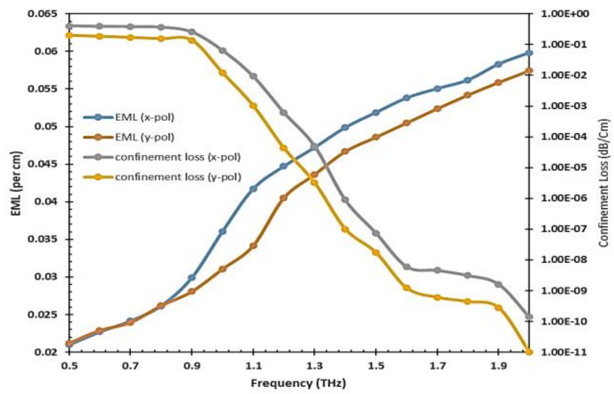

Figure 5. EML and Confinement loss of x-pol and y-pol mode versus frequency

Confiement loss is a crucial parameter any PCF design. The mathematical representation below illustrates how light loss can occur in the core region due to the specific structure of the photonic crystal fiber (PCF), which includes air holes within the cladding. The following equation shows the relationship between the velocity of light in the waveguide, frequency and the imaginary part of effective refractive index.

$$\alpha_{CL} = 8.686 \times \frac{2\pi f}{c} \times Im(\eta_{eff}) \quad (3)$$

From the above figure it can be understood that as the frequecny increases the confinement loss reduces indicating that the confinement of light in the core region is stronger. The minimum confinement loss obtained are 10^{-10} cm^{-1} and 10^{-11} cm^{-1} for x-polarizationa and y-polarization modes.

4. Conclusion

In conclusion, this research article introduces a novel design of a Topas-based photonic crystal fiber (PCF) with a rectangular air gap core containing slots, surrounded by cladding comprised of circular and octagon air holes. The arrangement of circular air holes forms a square and octagon lattice structure, while the octagon air holes create a rhombic lattice. The primary objectives of this study were to achieve an ultra-low effective mode area (EML), high birefringence, and very low confinement loss, all tailored to specific frequency ranges. The proposed PCF structure shows great promise for 5G applications due to its unique combination of properties and functionalities. In future, more waveguide properties like core power fraction, dispersion, spot size and V-parameter can be studied in connection to varying core diameter and porosity to gauge the preformance in much better way.

Author Contributions: Sandip Das was responsible for generating concepts, conducting simulations, and preparing the initial draft of the paper. Riya Sen took on the role of optimizing the simulated design, editing the paper, and preparing the final draft. Ultimately, Sandip Das and Riya Sen collaborated to finalize the paper. All authors have read and agreed to the published version of the manuscript."

Funding: This research received no external funding.

Data Availability Statement: No external data or new data is created.

Conflicts of Interest: The authors declare no conflict of interest.

References

1. Carr GL, Martin MC, McKinney WR, Jordan K, Neil GR, Williams GP. High-power terahertz radiation from relativistic electrons. Nature. 2002 Nov 14;420(6912):153-6. doi: 10.1038/nature01175. PMID: 12432385.
2. Pinto, Ana M. R., Lopez-Amo, Manuel, Photonic Crystal Fibers for Sensing Applications, Journal of Sensors,2012,1687-725X, https://doi.org/10.1155/2012/598178.
3. Zhang J, Grischkowsky D. Waveguide terahertz time-domain spectroscopy of nanometer water layers. Opt Lett. 2004 Jul 15;29(14):1617-9. doi: 10.1364/ol.29.001617. PMID: 15309837.
4. Skorobogatiy, M., Dupuis, A.: Ferroelectric all-polymer hollow Bragg fibers for terahertz guidance. Appl. Phys. Lett. 90(11), 113514 (2007). https://doi.org/10.1063/1.2713137
5. Hasan, M.R., et al.: Polarization-maintaining low-loss porous-core spiral photonic crystal fiber for terahertz wave guidance. Appl. Opt. 55(15), 4145–4152 (2016). https://doi.org/10.1364/AO.55.004145
6. Nagatsuma, T., Ducournau, G., Renaud, C.: Advances in terahertz communications accelerated by photonics. Nat. Photon. 10(6), 371–379 (2016). https://doi.org/10.1038/nphoton.2016.65
7. Atakaramians, S., et al.: Terahertz dielectric waveguides. Adv. Opt. Photon. 5(2), 169–215 (2013). https://doi.org/10.1364/AOP.5.000169
8. Dupuis, A., et al.: Transmission measurements of hollow-core THz Bragg fibers. J. Opt. Soc. Am. B 28(4), 896–907 (2011). https://doi.org/10.1364/JOSAB.28.000896
9. Nagel, M., Marchewka, A., Kurz, H.: Low-index discontinuity terahertz waveguides. Opt. Express 14(21), 9944–9954 (2006). https://doi.org/10.1364/OE.14.009944
10. Uthman, M., et al.: Design and characterization of low-loss porous-core photonic crystal fiber. IEEE Photon. J. 4(6), 2315–2325 (2012). https://doi.org/10.1109/JPHOT.2012.2231939
11. Islam, S.: Design and analysis of advanced photonic devices for electromagnetic transmission and sensing. Ph.D. thesis, Faculty of Engineering, University of Adelaide, Australia (2021)
12. Hasan, M.R., Islam, M.A., Rifat, A.A.: A single mode porous-core square lattice photonic crystal fiber for THz wave propagation. J. Eur. Opt. Soc. Rapid Publ. 12(1), 15 (2016). https://doi.org/10.1186/s41476-016-0017-5
13. Hasan, M.R., et al.: Low-loss and bend-insensitive terahertz fiber using a rhombic-shaped core. Appl. Opt. 55(30), 8441–8447 (2016). https://doi.org/10.1364/AO.55.008441
14. Hasan, M.R., et al.: Dual-hole unit-based kagome lattice microstructure fiber for low-loss and highly birefringent terahertz guidance. Opt. Eng. 56(4), 043108 (2017). https://doi.org/10.1117/1.OE.56.4.043108